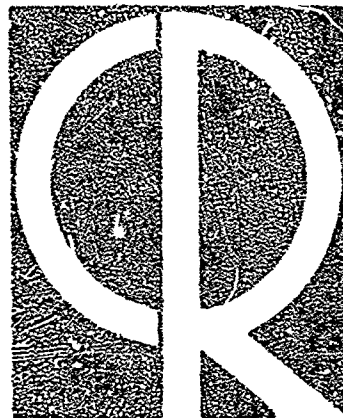




AD626694



Research Report

Code 1

CLEARINGHOUSE
FOR FEDERAL SCIENTIFIC AND
TECHNICAL INFORMATION

Hardcopy - Microfilm

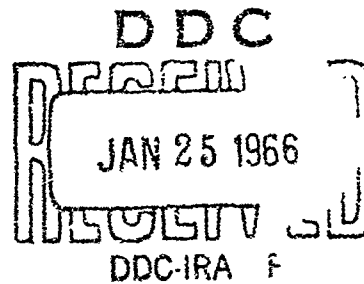
3.00 + 2.50 26-1001

ARCHIVE COPY

PROCESSING COPY

Electron Density Profiles of Wavemotions in the Ionosphere Caused by Nuclear Detonations

GEORGE J. GASSMANN



X

Research Report

Electron Density Profiles of Wavemotions in the Ionosphere Caused by Nuclear Detonations

GEORGE J. GASSMANN

Abstract

Horizontally traveling waves in the ionosphere, occurring naturally and from nuclear detonations, cause nonvertical reflections and, therefore, abnormal ionospheric recordings at stations during overhead passage. It is shown how an electron density cross-section in the vertical plane through an ionospheric wave can be constructed from a single station's ionospheric recordings, provided those are taken at time intervals not exceeding 5 minutes and provided the general direction of travel is known. The described analysis yields also an approximate value for the velocity. Figures 6 and 7 show examples of profiles of ionospheric waves from two different nuclear detonations, observed at great distances. The ionospheric wave of 30 October 1961 from Novaya Zemlya appears to be caused by a gravity wave, as may be inferred from Table 3 which gives a review of world-wide observations.

Acknowledgements

This research has been sponsored in part by the Defense Atomic Support Agency, Washington, D. C. The airborne ionograms were produced under the supervision of R. Gowell of AFCRL, with Major R. Creager of the 3245th Operations Group, L. G. Hanscom Field, Bedford, Massachusetts as aircraft commander. Helpful discussions were held with T. Barrett of American Science and Engineering, Inc., Cambridge, Massachusetts.

Contents

	Page
List of Illustrations	vi
List of Tables	vi
1 INTRODUCTION	1
2 THE RAW DATA	2
3 THE ELECTRON DENSITY PROFILES	10
4 ESTIMATE OF VELOCITY	10
5 CONSTRUCTION OF VERTICAL PROFILES OF IONOSPHERIC WAVES	13
6 DISCUSSION	15
References	21

Illustrations

Figure		Page
1	Outline Map - Novaya Zemlya Detonation (in both geographic and magnetic coordinates)	3
2a, b	Sequence of Ionograms Taken on Aircraft on 30 October 1961, 0850 to 0920 GMT	4, 5
3	Ionograms of Figure 2 Retraced, and Extraordinary Components and Multiples Eliminated	6
4	Outline Map - Bikini Detonation (in both geographical and magnetic coordinates)	7
5a, b	Sequence of Ionograms taken at Kusaie Island after the Bikini Detonation	8, 9
6	Cross-Section of Ionospheric Wave from Novaya Zemlya Passing over Aircraft. Dotted contour lines are not measured and represent suggested supplementation.	14
7	Cross-Section of Ionospheric Wave from Bikini Passing over Kusaie. Dotted contour lines are not measured and represent suggested supplementation.	15
8	Graphical Construction of Curved Ray Paths	16

Tables

Table		Page
1	The Ionograms of Figure 3 reduced to true 'height'	11
2	The Ionograms of Figure 5 reduced to true 'height'	12
3	Review of Observations on Ionospheric Wave of 30 October 1961	17

Electron Density Profiles of Wavemotions in the Ionosphere Caused by Nuclear Detonations

1. INTRODUCTION

Ionospheric h'f recordings, especially those taken at arctic stations, frequently during one 24-hour period show echoes that cannot be explained by assuming horizontally stratified layers. It has been obvious that some of the echoes are not strictly vertical soundings but arise from large-scale irregularities near the zenith of the station. From comparing consecutive h'f recordings it has also been obvious that many of those natural irregularities travel with a speed of the order of sound waves. The determination of dimensions, speed, and direction is possible, in principle, if one utilizes several sounding stations whose spacings are large enough to obtain, for triangulation, measurable differences in echo-ranges at each station and whose spacings are small enough to obtain recordings that can be correlated.

Such stringent experimental requirements for investigating natural large-scale movements in the ionosphere, requiring three ionospheric stations at close distance (100 km), are considerably eased for the case of man-made disturbances. In the latter case the direction of movement at a particular station and the speed of travel may be deduced approximately from the geographical location and the time where and when the man-made disturbance was introduced. With this information available the ionograms from a single station are sufficient to obtain a vertical cross-section of the ionospheric layers along the direction of travel at a time when the disturbance passes through. How this can be done is outlined below and is demonstrated by two examples. One is the wave from the nuclear detonation at Novaya Zemlya on 30 October 1961, as observed near Norway; the other example utilizes

(Received for publication, 8 March 1963)

ionospheric data taken at Kusaie Island, South Pacific, after a detonation above Bikini Atoll.

2. THE RAW DATA

The data on 30 October 1961 were taken from a USAF KC-135 jet aircraft at 67°N-10°E while on a heading toward magnetic north (Figure 1). The distance to Novaya Zemlya was approximately 1600 km. The yield of the detonation was estimated as being between 35 and 90 MT; and the altitude of the burst was estimated as being below the tropopause.¹ Burst time was 0833 GMT. The equipment in the aircraft consisted of a modified Step Frequency Ionospheric Recorder* that sweeps from 1 to 25 Mc in 100 kc steps within a 4-minute time period. Nominal transmitter output was above 10 kw. The transmitting-receiving antenna was of the traveling-wave type; three wires approximately 23 m long extended from a common tiepoint on the aircraft's upper fuselage to three separate points on the vertical stabilizer, each wire terminated by a resistor. The antenna pattern favored upward radiation in a wide cone of about 90° for most frequencies. Antenna efficiency was below but approaching that of the conventional delta antenna of an ionospheric ground station at most frequencies.

The sequence of ionograms on 35-mm film used in this analysis is reproduced in Figures 2a and 2b. The same ionograms retraced and supplemented, eliminating extraordinary component and multiples, appear in Figure 3.

Data from the Bikini detonation were taken at Kusaie Island 740 km south of Bikini (Figure 4).² The equipment was an Ionospheric Recorder Type C3, which swept the frequency range from 1 to 25 Mc within 30 sec, using a standard delta antenna. Detonation occurred approximately 1 hour before local sunrise. The detonation above Bikini Atoll was below the tropopause and equivalent to several megatons of TNT.

Figures 5a and 5c show the sequence of ionograms used in this analysis. This sequence covers the first disturbance arriving at Kusaie. (A second disturbance, not covered in this analysis, arrived overhead at Kusaie at H+56 minutes.)

* Manufactured by Philips Electronics Industries Ltd, Toronto, Canada

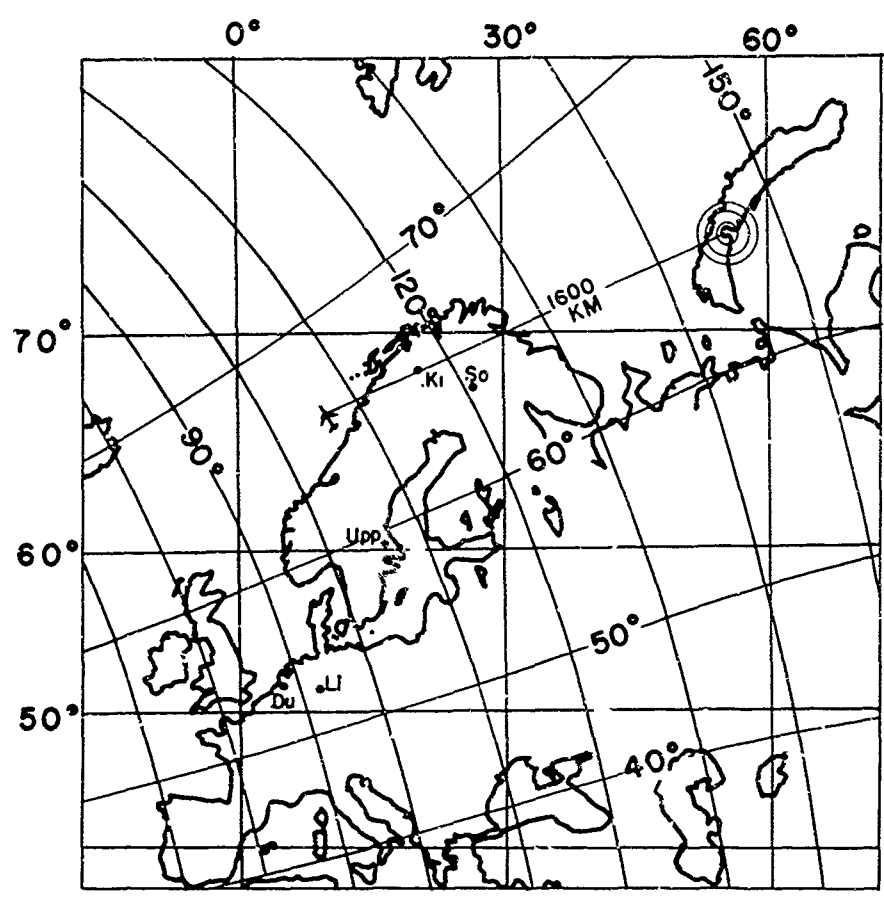


Figure 1. Outline Map - Novaya Zemlya Detonation (in both geographic and magnetic coordinates)

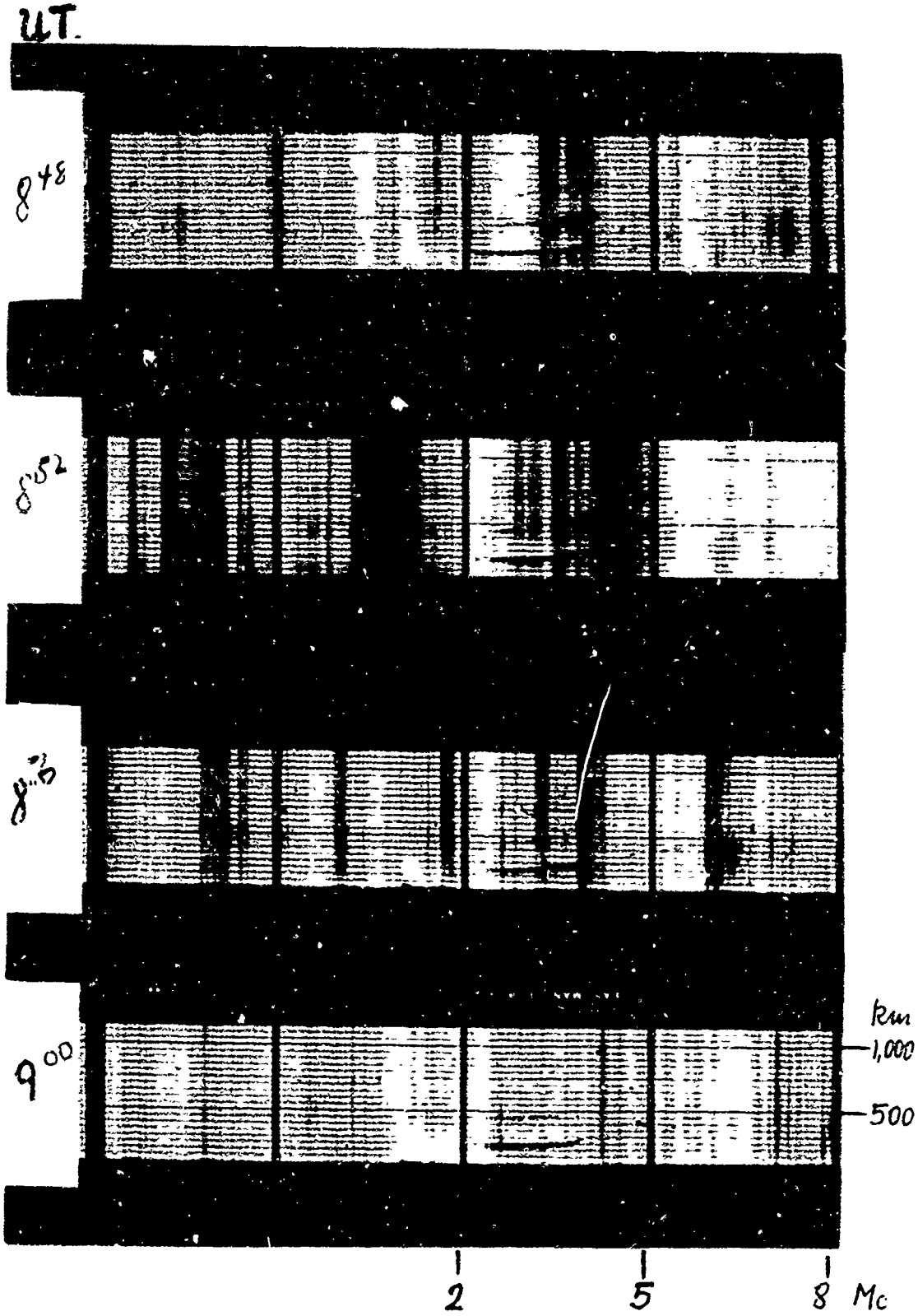


Figure 2a. Sequence of Ionograms taken on Aircraft on 30 October 1961, 0850 to 0920 GMT

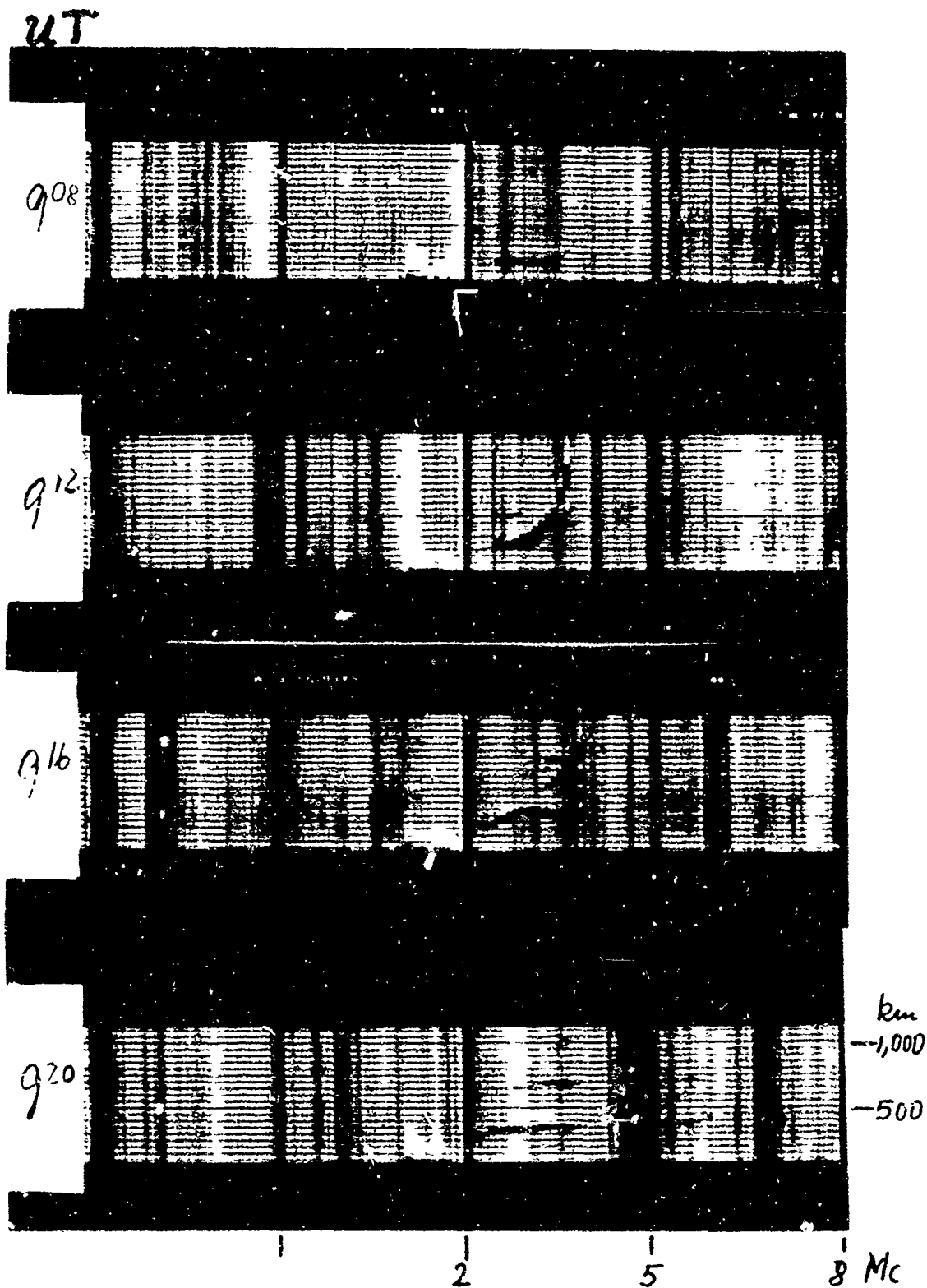


Figure 2b. Sequence of Ionograms taken on Aircraft on 20 October 1961, 0850 to 0920 GMT

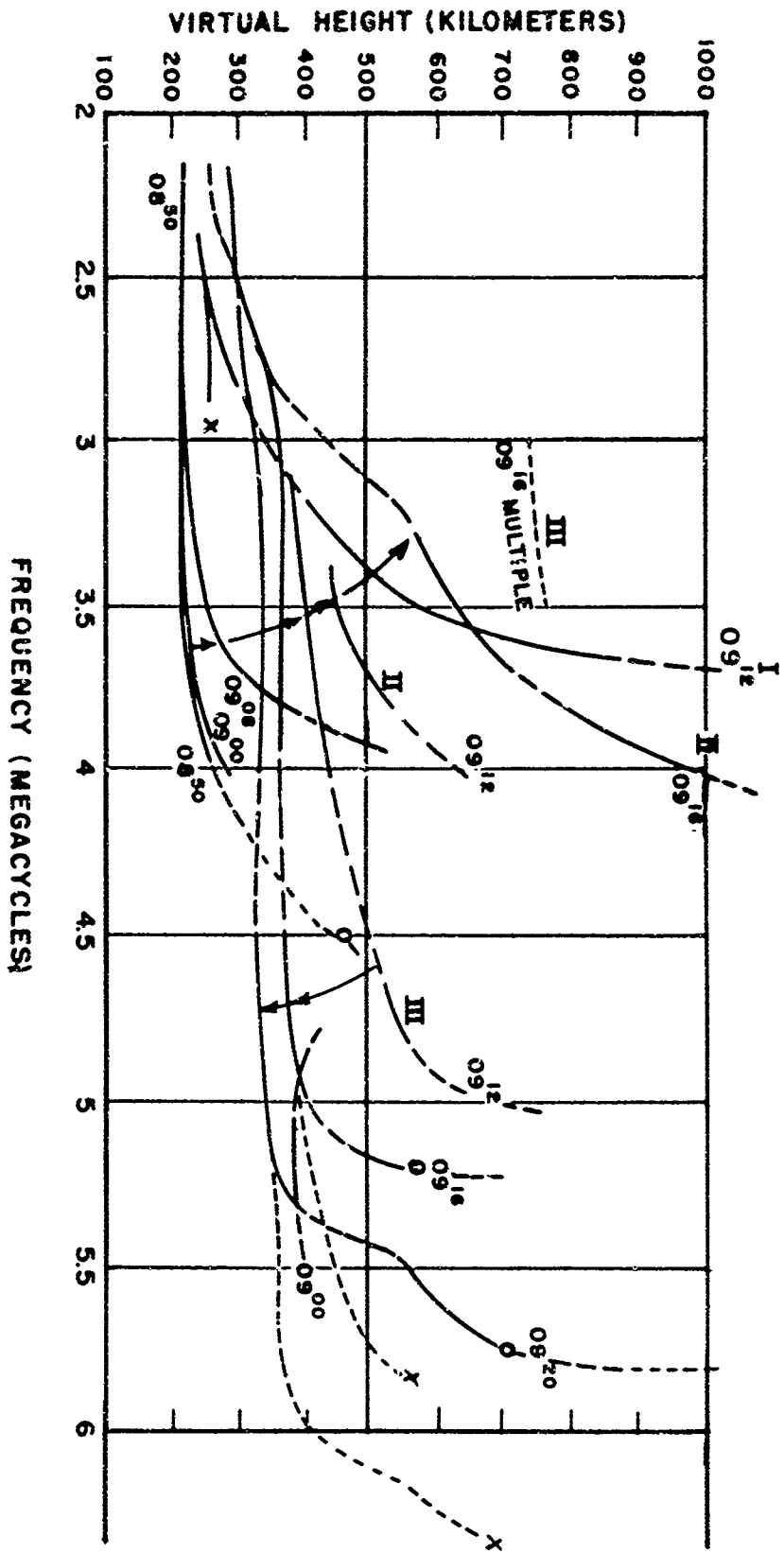


Figure 3. Ionograms of Figure 2 Retraced, and Extraordinary Components and Multiples Eliminated

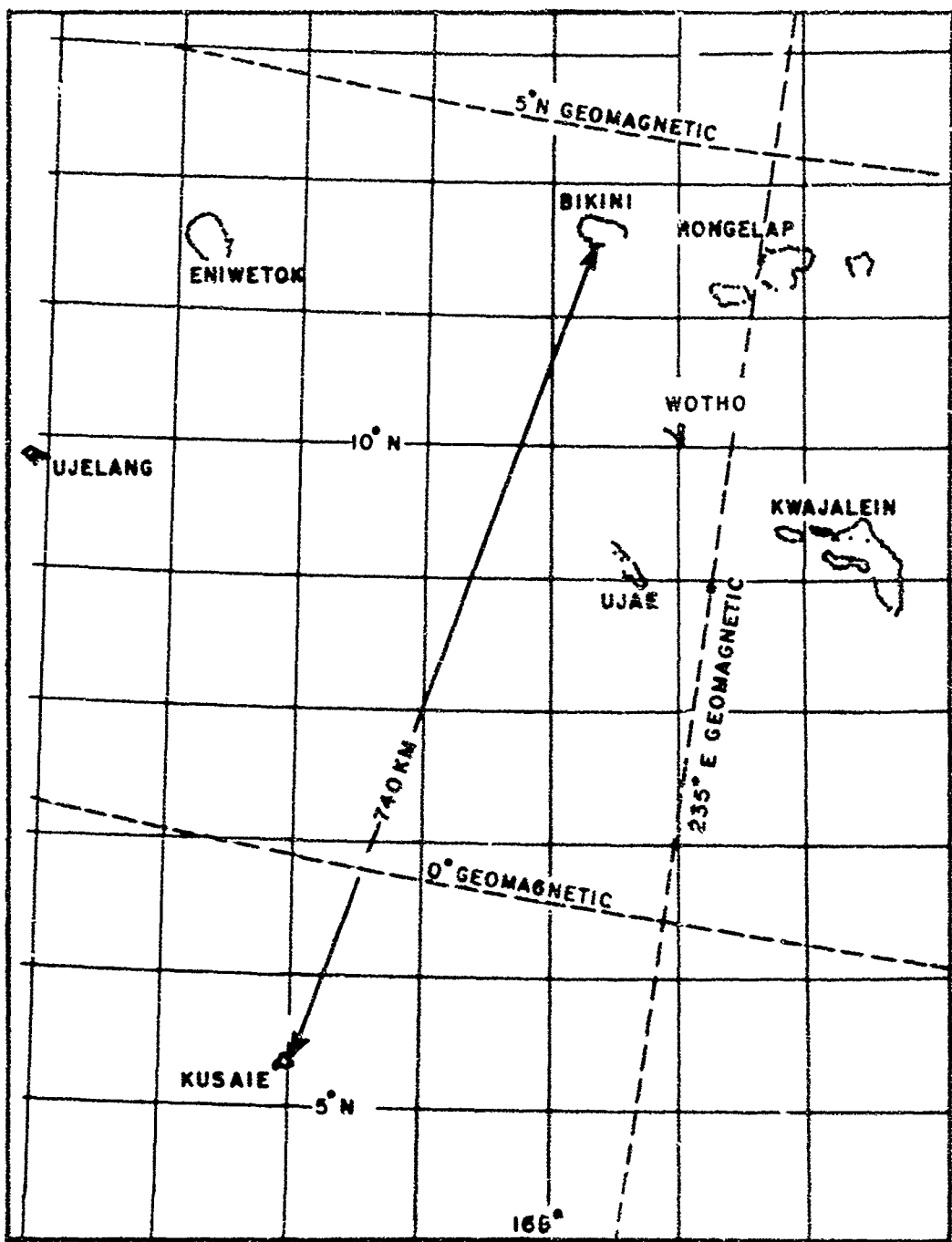


Figure 4. Outline Map - Bikini Detonation (in both geographical and magnetic coordinates)

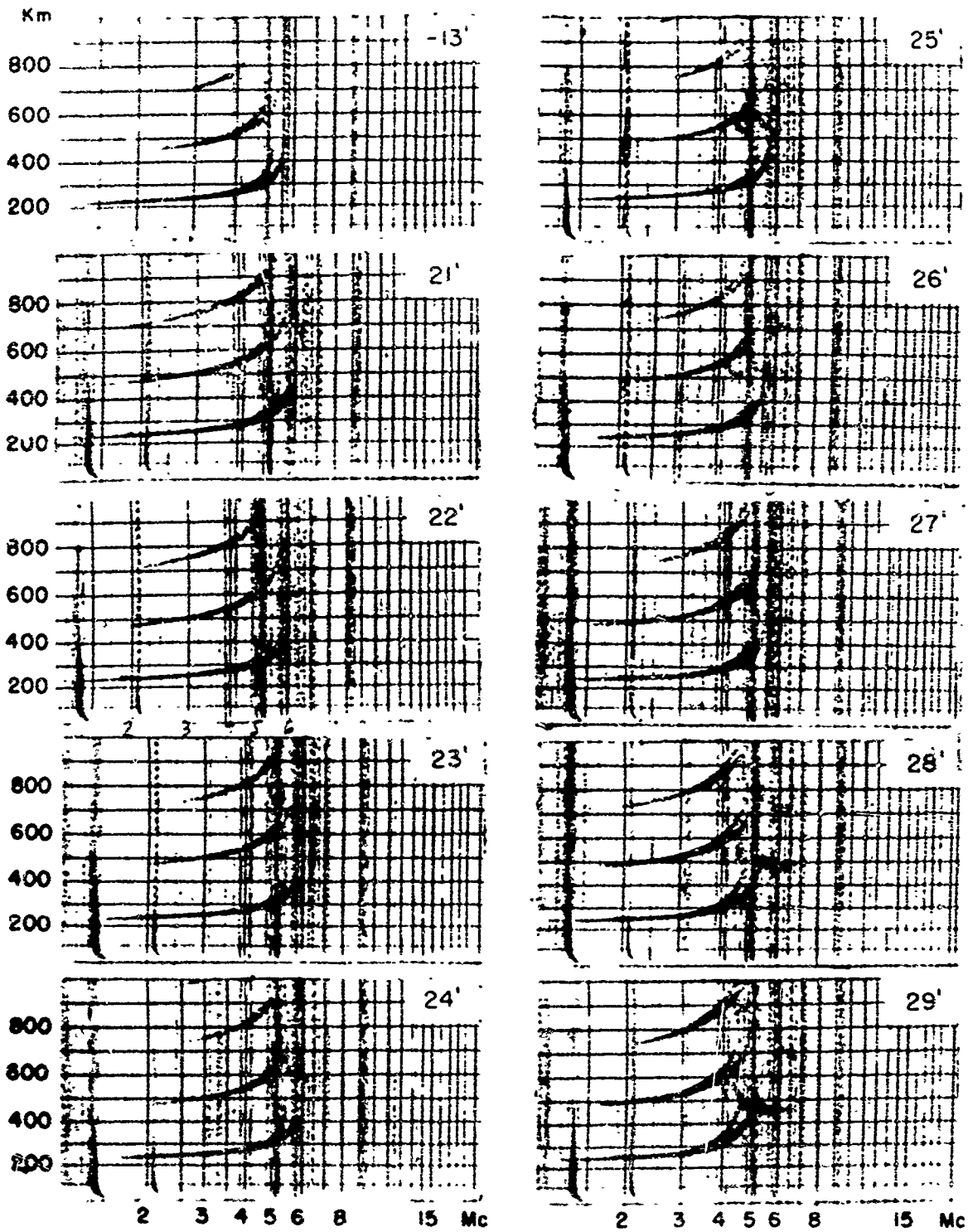


Figure 5a. Sequence of Ionograms taken at Kusaie Island after the Bikini Detonation

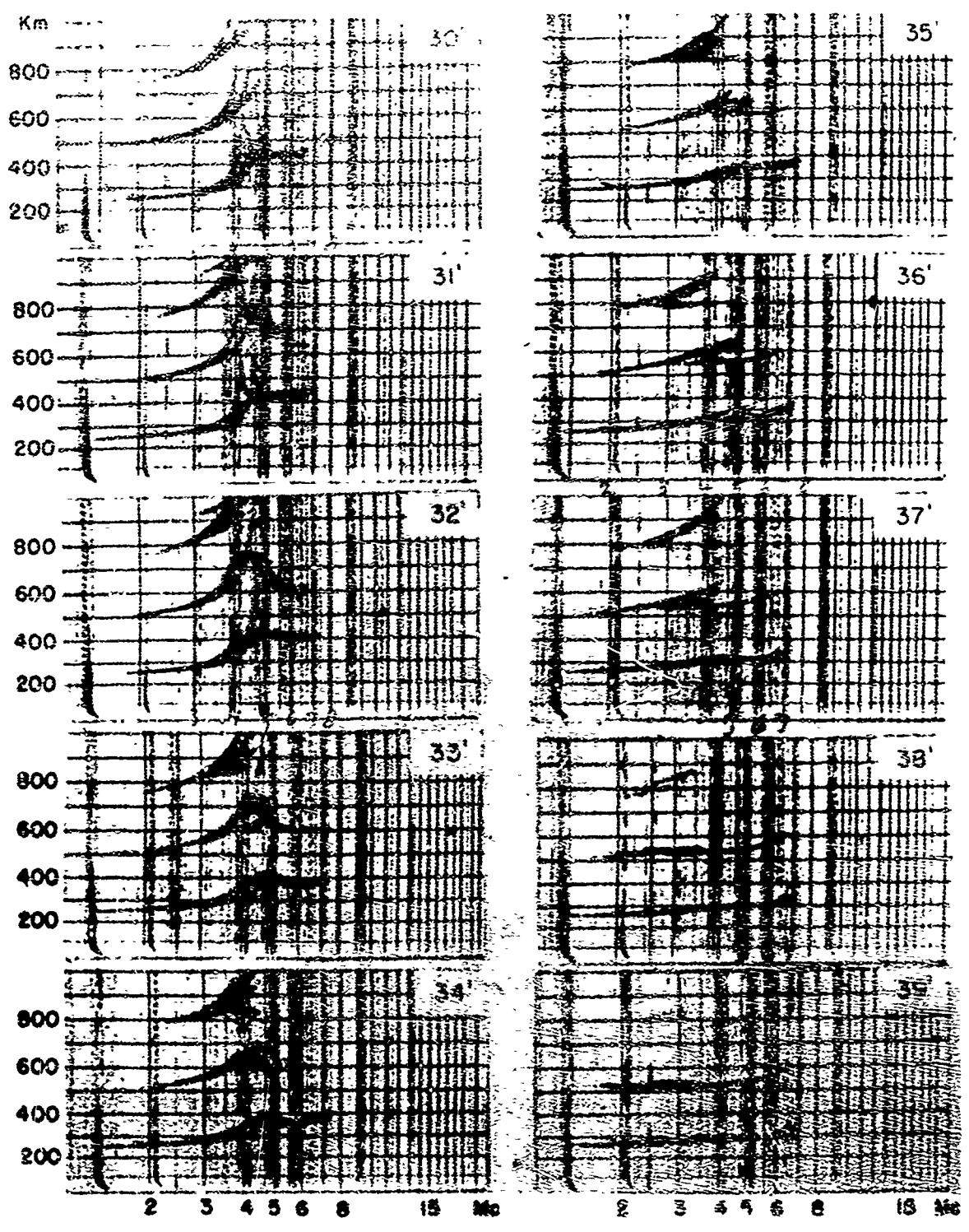


Figure 5b. Sequence of Ionograms taken at Kusaie Island after the Bikini Detonation

3. THE ELECTRON DENSITY PROFILES

The reproduced sequences of ionograms show that the single echo traces near the start of the sequence develop into two or sometimes more branches (marked I, II, and III on Figure 3). This means that for certain frequencies reflections occur at more than one distance. This indicates clearly the existence of separate ray paths for each reflection at one particular frequency, since in one single ray path the closest reflection surface would obscure all others at a farther distance. (Non-obscuring partial reflections, which produce echoes at virtual ranges lacking the feature of critical frequency and associated range increase (cusp), are not seen on the ionograms and are not considered here.) Each branch in the ionograms is the result of a particular set of ray paths (from the station to the reflection level and back). Each set may consist of a bundle of single rays. For simplification, however, it has been assumed that each branch is created in the same way as are vertical ionograms, i.e., the ray paths for all frequencies of a branch are identical except for different penetration heights into the layers. With this simplification, reducing the cone angle of the bundle of ray paths to zero, each branch of the ionogram traces can be reduced from virtual to true height. This procedure is standard for vertical ionograms and is done with the notion that the obtained true 'height' is actually the distance to the layer at an unknown elevation angle. For the reduction to true height the simple method of Kelso³ was used since it allows rapid hand calculations and yields sufficient accuracy compatible with that of the other steps in the analysis.

Tables 1 and 2 contain results of the true height reduction, referring to the ionograms of Figures 3 and 5, respectively.

4. ESTIMATE OF VELOCITY

The next step in this analysis is the postulation that the irregularity travels horizontally as a whole and with a particular velocity. The better this is fulfilled and the better the velocity is estimated, the faster the analysis described under Section 5 leads to results.

The effect of the Novaya Zemlya detonation on the ionospheric recordings at the aircraft shows up first at 0900 GMT. This yields an average speed of 1600 km/27 min or 987 m/second. On the other hand, other widely-differing velocity values ranging from 330 to 910 m/sec from ground observation were measured (Table 3 page 17). From these data it appeared obvious that the ionospheric disturbance had started with higher velocity, slowing down at medium distances, and that the aircraft happened to be flying at a transition distance. The analysis, therefore, had been started with

TABLE 1 Ionograms of Figure 3 reduced to true height s

GMT	Plasma-frequency												
	f_N 2.0	3.0	3.5	3.7	4.0	4.5	5.0	5.5	5.7	5.8			
0852	210	215	220		230	280	---						
0900	210	215	220		230		295	330	---				
0908	210	215	220		---								
	Branch												
	Branch I												
0912	230	240	320	370	---		370						
	Branch II												
	230	240	300		320		390	---					
	Branch III												
0916	255	295	390	410	490	---							
	Branch II												
	255	295	310		320		330		400			---	
	Branch III												
0920	270	300	305		310		320		360			385	
	true 'height' s												
	km												

Conversion: f_N^2 [Mc] = $7.98 \times 10^{-5} N_e$ [electrons/cm³]

TABLE 2. Ionograms of Figure 5 reduced to true height s

Minutes After detonation	Plasma-Frequency										
	f_N	2.0	.3.0	4.0	5.0	5.1	5.3	6.0	6.4	6.5	6.8
12		215	230	240	265	---					
22		230	240	250	280	290	315	---			
24		235	245	250	290	320	---				
26	Branch II	240	250	260	290	---		360	---		
	Br: h III										
28	Branch II	245	260	270	330	---		360		390	---
	Branch II										
30	Branch II	255	265	280	---					375	---
	Branch III			320	340						
32	Branch II	260	270	290	---			340	345		360
	Branch III				320						
34		260	270	290	310			320	330		350
36		260	270	285	300			310	---		
38		265	275	280	295			305	315		340
46		240	250	255	260			280	---		

Conversion: f_N^2 [Mc] = $7.98 \times 10^{-5} N_e$ $\left[\frac{\text{electrons}}{\text{cm}^3} \right]$

true height' s

km

an estimated velocity of 670 m/sec which, however, yielded inconsistent results. Several lower velocities down to 420 m/sec were then assumed, and it was found that most consistent results were obtained with a velocity of 500 m/second.

The arrival at Kusaie of the ionospheric disturbance from the Bikini detonation yielded an average speed of 514 m/second. In the analysis, however, consistent results were obtained with velocities centering at 420 m/second.

5. CONSTRUCTION OF VERTICAL PROFILES OF IONOSPHERIC WAVES

Figure 6 presents a two-dimensional coordinate system showing vertical distances above ground and horizontal distances from an arbitrary zero-point. The abscissa also shows the time when ionospheric records were taken. The relative position of the time marks to the kilometer marks on the abscissa is arbitrary, however, the value $\partial(\text{distance})/\partial(\text{time})$ equals 500 m/sec representing the speed postulated above. The zero-km mark on the abscissa may be considered as being fixed with the horizontally-moving ionospheric disturbance; the ionospheric station consequently moves along the zero height mark from left to right. The true height values (s of Table 1) were now plotted as segments of circles, with that particular radius above that point on the ground which is marked with the particular time when the record was taken. After all values of Table 1 were plotted in this manner, a first generation of contour lines of the plasma frequency f_N was drawn by connecting all segments of circles of the same plasma frequency by smooth curves. Several inconsistencies remained, especially in the upper levels of f_N , because in this illustration each ray path from the ionospheric station to the reflection point is represented by a straight line, namely, the radius of the particular segment to the point where it touches the contour line.

A second generation of contour curves was then obtained by replacing those straight ray paths of obviously incorrect shape with curved ones. Samples of curved ray paths were obtained by a graphical construction according to Figure 8, which is based on Snell's Law and which approximates the refraction process by a step-wise procedure. The demand for sample ray paths can be kept to a minimum if one is experienced in selecting ray paths (choosing the right departure angle) whose reflection points are both consistent with others and which approximately fulfill the specular reflection requirement (180° return). The drawing of the contour lines is then a matter of interpolation.

A third generation of contour lines may now be obtained, commencing at the lowest levels of uncertainty and proceeding to higher levels, by calculating the virtual height $s' = \sum^s \frac{ds}{\mu}$ along each ray path. If this value differs by $\Delta s'$ from the experimental s' ('virtual height'), the entire procedure might be repeated with new values

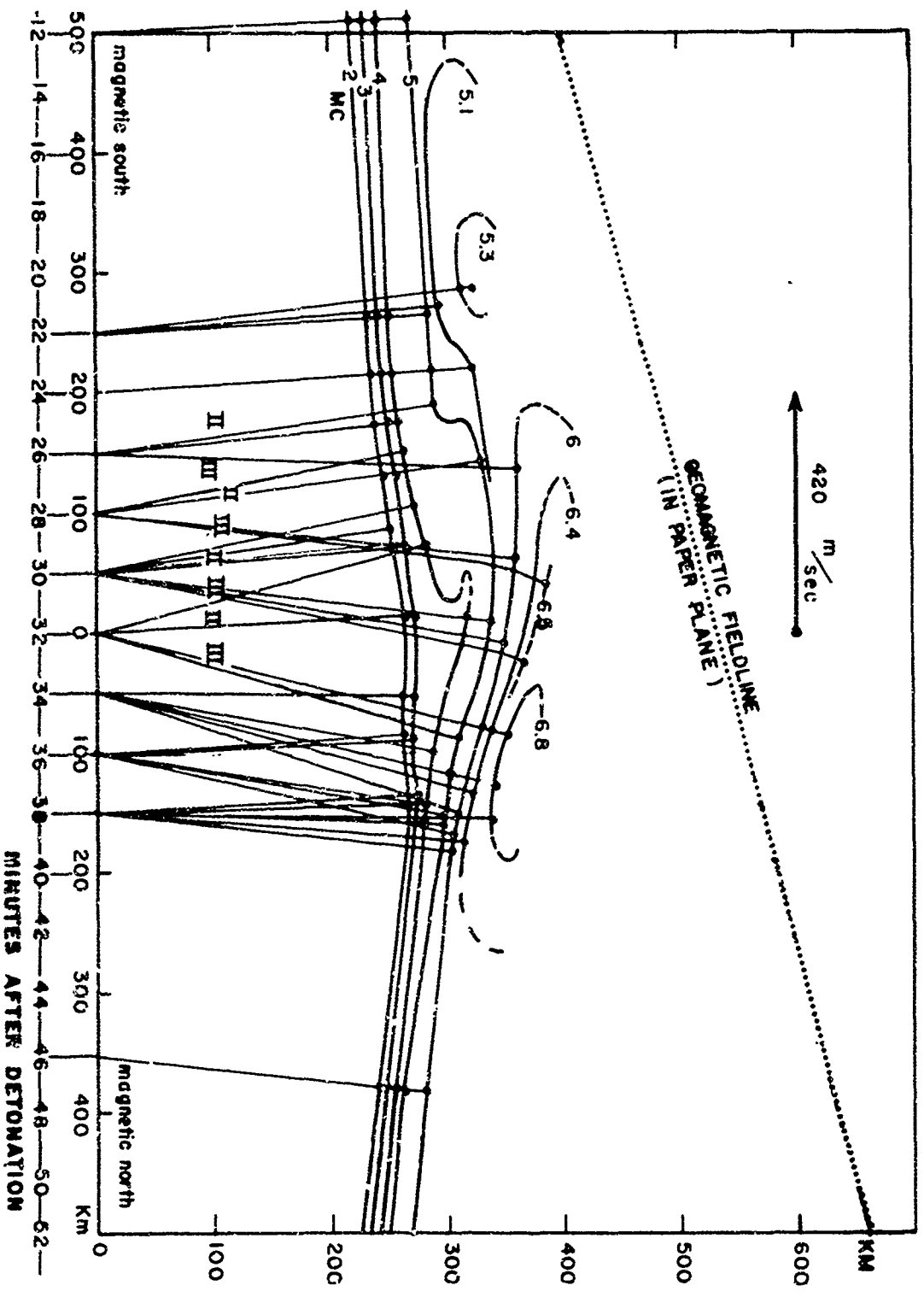


Figure 7. Cross-Section of Ionospheric Wave from Bikini Passing over Kusaie. Dotted contour lines are not measured and represent suggested supplementation.

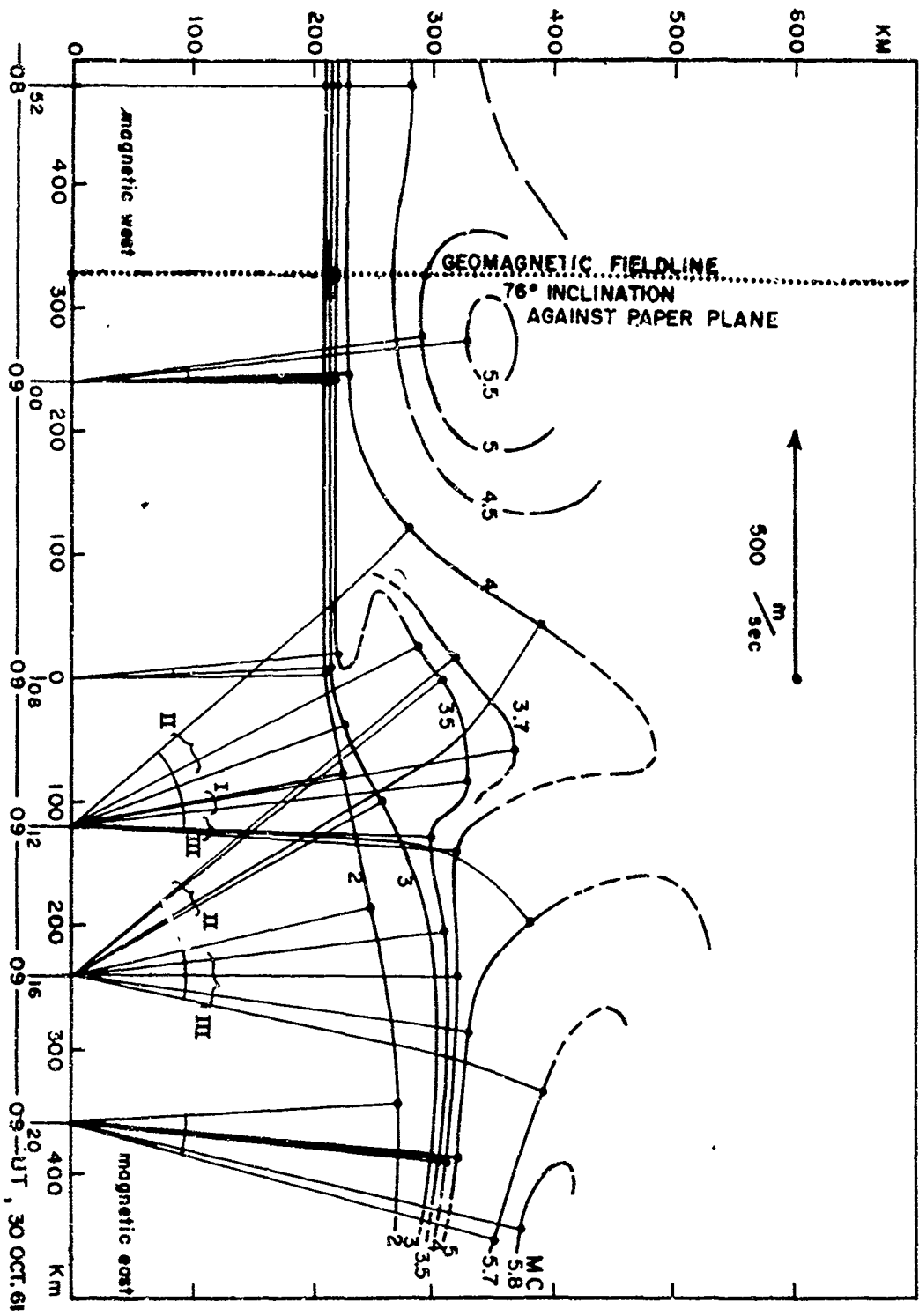


Figure 6. Cross-Section of Ionospheric Wave from Novaya Zemlya Zemlya Passing over Aircraft. Dotted contour lines are not measured and represent suggested supplementation.

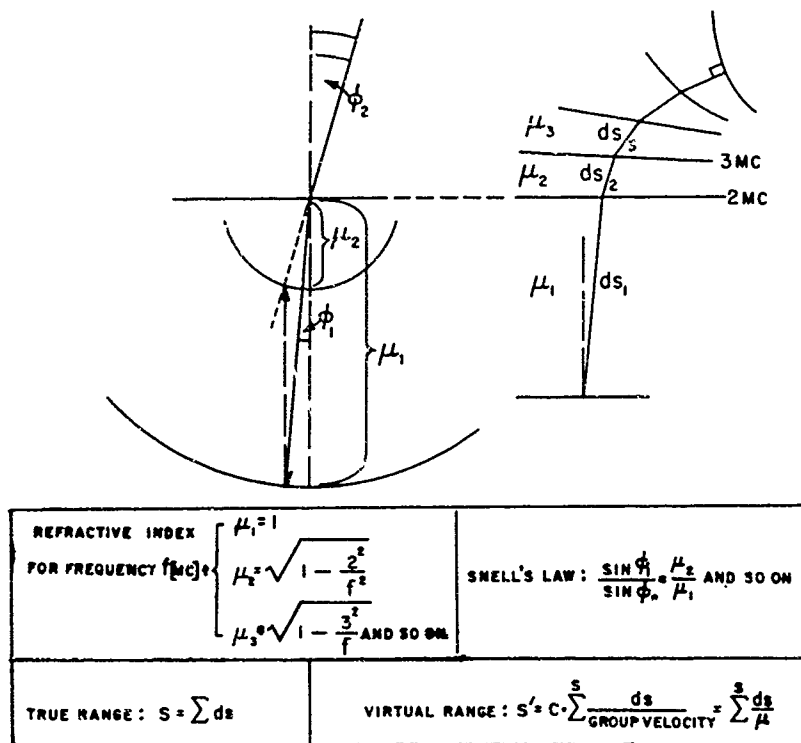


Figure 8. Graphical Construction of Curved Ray Paths

of s individually adjusted according to $\Delta s'$. This refinement was used here on only a few points as a check.

The described construction assumed a velocity of 500 ± 80 m/second. In trials with velocities beyond these limits certain inconsistencies could not be removed.

The ionospheric wave over Kusaie was constructed in the same way. The tabulated values of Table 2 yield contour lines as seen in Figure 7, in which a velocity of 420 ± 80 m/sec is assumed. Assuming velocities beyond the indicated limits led to inconsistencies during the construction of the contour lines.

The above described construction of contour lines may be applied to any sequence of ionospheric recordings. As a general rule, however, it is felt the time interval between recordings should not exceed 5 minutes.

6. DISCUSSION

The traveling ionospheric disturbance from the 30 October 1961 detonation has been observed at several locations. Table 3 shows a review of the results with velocities deduced from the various data and assumptions. The values bear varying validity margins caused by the uncertainties of distance and travel time. The determination of the latter is affected by the period of data taking and by the uncertainty

TABLE 3. Review of observations on ionospheric wave of 30 October 1961

Source	Location	Results	Approx. Distance to Novaya Zemlya, (km)	Average Velocity of F Layer Disturbance (m/sec)
Oksman ⁴	Sodankyla ¹¹	Sudden change of f_oF_2 at H+22 min	1,200	910
Rose, et al. ⁵	Sodankyla ¹¹	Disturbance of F layer 26.3 hr after detonation (round-the-world NE). Disturbance of F layer 27.2 hr after detonation (round-the-world SW) Microbarographic (round-the-world) signal travels at a speed of 311 m/sec On magnetometers no pronounced effect noticed during ionospheric disturbance.	40,000-1,200	413
Lindqvist ⁶	Kiruna	Sudden change of f_oF_2 at H+24 min	1,350	938
Hultqvist et al. ¹	Kiruna	In addition to the above: at H+25 hr strong disturbance of F layer (attributed to N. Z. detonation of 31 Oct 62, 0830 UT) If interpreted as round-the-world.	40,000-1,350	430
Stoffregen ⁷	Kiruna, Lykseele, Uppsala, Lindau, Dourbes, Athens	Sudden change of f_oF_2 with consecutive oscillations, period/hr increasing with distance. Amplitudes Δf_oF_2 increasing with distance.	630 onset (430) 1st max (260) 2nd max (170) 3rd max	
Dieminger et al. ⁸	Lindau	Marked change of f_oF_2 (1/2 hr records) consecutive oscillations of f_oF_2 , period approx. 1.5 hr Disturbance of F layer 31.5 hr after detonation (round-the-world, NE or SW uncertain).	3,200	460 to 610
Gardiner ⁹	Reykjavik, Lulea, Inverness, Uppsala, Slough, Lindau, Roma	Amplitudes Δf_oF_2 increasing with decreasing magnetic latitude. Microbarographic (round-the-world) signals appear to travel at velocities $v_{west} = 296$ m/sec and $v_{east} = 314$ m/sec	40,000-3,200 40,000+3,200	330 380
Obayashi ¹⁰	Osaka, Sodankyla, Tromso, Kiruna, Uppsala, Lindau,	Disturbances of F layer, period > 10 min Excessive velocity near detonation, then nearly constant.		420

TABLE 3. (Contd)

Source	Location	Results	Approx. Distance to Novaya Zemlya, (km)	Average Velocity of F Layer Disturbance m/sec
Lichtman et al. 11	Dourbes, Schwarz, Roma, Wakaunai, Akita, Yamagawa	Wavelength in F layer approx. 200-300 km, (Gravity Wave). No marked changes in F2 at North American Stations. Microbarographic (round-the-world) signals travel at 310 m/sec		370 to 820
Gassmann (Figures 2a and 6)	Same stations as analyzed by Obayashi plus Quetta, Munderaring, and Kerguelen	Decrease of f_oF_2 followed by oscillations, period: 1.5 to 2.5 hr. No effect of geomagnetic field on propagation of F layer disturbance noticeable.		
Gassmann (Figures 2a and 6)	KC135 near Norway	Sudden indication of F layer disturbance at H+27 min	1,600	987
		Profile analysis from sequence of ionospheric soundings.		500±80
<u>OTHER RELATED OBSERVATIONS</u>				
Gassmann (Figures 5a and 7)	Kusaie, Bikini Detonation	Sudden indication of F layer disturbance at H+24 min	740 to Bikini	514
		Profile analysis from sequence of ionospheric soundings.	740 to Bikini	420±80
Matsushita ¹²	Maui, Orange Detonation 12 Aug 58	Change of f_oF_2 .	1,300 to Johns-ton	900
Cummack et al. 13	Magn. Observations in Pacific. Peak Detonation 1 Aug 58	F layer disturbance inferred from magnetic observations.		500 to 2,500

of the time of origin. If, for example, the ionospheric wave was originated by the rising fireball, a delay after detonation of as much as 5 minutes should be assumed, raising some of the velocities listed to even higher values.

The F-layer disturbance appears to have started with a velocity exceeding 1000 m/sec, slowing down after a few thousand kilometers of travel to velocities between 330 and 430 m/second. Simultaneously, a microbarographic wave propagated to far distances at lower velocities near 300 m/sec as a separate phenomenon. The F-layer disturbance consisted of a sudden onset followed by consecutive oscillations that lasted for several hours. The wave appears to have excluded certain directions of propagation; this might explain the discrepancy in the round-the-world velocity values that are based on great circle paths. The observations of Stoffregen and of Gardiner, namely, the increase of the amplitude of the wave with distance and/or with decreasing magnetic latitude, appear significant.

The observed wavelength of $\gg 100$ km indicates that compressional forces play a minor role in this wave since only acoustic waves of frequencies > 0.03 cps or of wavelength < 100 km can propagate.¹⁴ Obayashi suggests that the ionospheric disturbance was caused by a gravitational wave.¹⁰ Such a wave would have large amplitudes at great heights. However, at F-layer maximum and above, the coupling of motion of neutral and charged particles is appreciable and imposes an attenuation on the gravity wave. By this effect Obayashi explains why the largest amplitude of the wave is observed in the lower F layer.

It is obvious that, under the influence of either a gravity wave or a compressional wave, the motion of the F-layer plasma will not coincide with that of the neutral particles, the former creating dynamo currents and/or electric fields. The cross-sections shown in Figures 6 and 7 must therefore be regarded as mere examples of a variety of possible forms. It must be expected that the shapes of the ionization contour lines will vary greatly, depending on the orientation of the geomagnetic vector relative to the direction of propagation.

References

1. Hultquist, B., Egeland, A., Gustafsson, G., Liszka, L., Ortner, J., Heikkila, K. E., Olsen, S., Makitalo, T., and Eriksson, B., "Report on Observations Made at Kiruna Geophysical Observatory During the Series of Nuclear Weapon Tests Carried Out at Novaja Zemlja Between 10 Sept and 4 Nov 1961," Kiruna Geophysical Observatory, Kiruna C, Sweden Scientific Report No. KGO 611, (11 Dec 1961).
2. Data taken in 1956 during Operation Redwing by Harris, A. K., Gassmann, G. J., Daniels, F. B., Pfister, W., Caplan, P. J., and Winkelman, R. E.
3. Kelso, J., "A Procedure for Determination of the Vertical Distribution of the Electron Density in the Ionosphere," Journ. Geoph. Res. 57, 357 (1952).
4. Oksman, J., Geophysical Observatory, Sodankyla, Finland, private communication.
5. Rose, G., Oksman, J., and Kataja, E., "Round the World Sound Waves Produced by the Nuclear Explosion on 30 October 1961 and Their Effect on the Ionosphere at Sodankyla," Nature, 192, 1173 (1961).
6. L'adquist, R., Research Institute of National Defense, Stockholm 80, Sweden, private communication.
7. Stoffregen, W., "Ionospheric Effects Observed in Connection with Nuclear Explosions at Nova Semlja on 23 and 30 October 1961," Res. Inst. of Nat'l Defense, Stockholm 8G, Sweden, Report FOA3/A517, (May 1962).
8. Dieminger, W. and Kohl, H., "Effects of Nuclear Explosions on the Ionosphere," Nature, 193 (No. 4819), 963 (Mar 1962).
9. Gardiner, G. W., "Effects of the Nuclear Explosion of 30 October 1961," Jour. Atm. Terr. Ph. 24, 990 (Nov 1962).
10. Obayashi, T., "Wide-Spread Ionospheric Disturbances Due to Nuclear Explosions During October 1961," Nature, 196, 4849 (Oct 1962).
11. Lichtman, S. W. and Anderson, E. J., "Ionospheric Effects of Nuclear Detonations in the Atmosphere," Hughes Aircraft Company, Culver City, California, Report OP-36.
12. Matsushita, S., "On Artificial Geomagnetic and Ionospheric Storms Associated with High-Altitude Explosions," Jour. Geophys. Res. 64, 1149 (1959).
13. Cummack, C. H. and King, G. A. M., "Disturbances in the Ionospheric F-Region following the Johnston Island Nuclear Explosion," Nature 184, 33 (Sept 1959).
14. Eckart, C., Hydrodynamics of Oceans and Atmospheres, Pergamon Press, New York (1960).